Arch. Metall. Mater. **69** (2024), 1, 325-336

DOI: https://doi.org/10.24425/amm.2024.149097

K. RAMKUMAR[1], K.A. SELVARAJAN[2], C. SATHIYA NARAYANAN[2], A. BOVAS HERBERT BEJAXHIN[3*]

PERFORMANCE ANALYSIS OF MULTI-POINT INCREMENTAL FORMING TOOL USING MARTENSITIC AISI 420 SHEET METALS

Incremental Sheet metal Forming (ISF) Process is a suitable process which helps to produce various parts used in automotive sector by rapid prototyping. This method of producing a prototype helps industry in reducing the production cost. In ISF process, a final product is evolved through local deformation of the sheet metal made by the tool. Usually better formability is obtained when the tool makes a better contact with the sheet metal throughout the process. Improved formability elevates dimensional accuracy of the product, thus increases the market value of the product. A new tool with multiple ball ends capable of making multiple mating points over sheet metal was used in this research to enhance the efficiency of formability and surface finish. Ability of the new Multi-Point Incremental Forming Tool (MPIF) was investigated and compared to the existing Single Point Forming Tool (SPIF) based on the formability and surface finish. Forming Limit Diagram (FLD), Strain Distribution (SD) and Scanning Electron Microscope (SEM) were used to examine the formability of the sheet metal. The SEM & 3D-Surface roughness profilometer were used to observe the sheet metals surface finish. In addition to these experimental techniques a simulation results were also used to predict the stress and strain rate during forming process. The experimentation and simulation outcome shows that the MPIF provides superior formability and surface finish.

Keywords: Incremental sheet metal forming; Formability analysis; AISI 420; Strain measurement; 3D-Surface roughness; Deform 3D

1. Introduction

Among the emerging technologies, ISF is one of the important processes used in small scale industries for rapid production without a huge investment [1]. The ISF does not require any specialized die to make a product like any other manufacturing process. In ISF process the product furnished is first designed using modelling software and then, by using CAM software a program is generated. The program should contain the details of tool movement like feed, speed, Vertical Step Depth (VSD). The generated CAM program is fed into the Computer Numerical Control (CNC) machine which controls the movement of tool. It also acts as a key factor to improvise the final outcome of the product. This forming tool travels in X, Y and Z axes to form the sheet metal resting on the forming fixture. The tool should make a proper contact with the sheet metal to give a better result. Two types of tool were extensively used in the incremental forming process namely ball ended and hemispherical ended tool. Among these two, ball ended tool gives better output compared to hemispherical tool due to its better rolling contact on the sheet metal [2,3]. Here the frictional effect of the tool also plays a significant role in improving the formability and surface finish [4]. Various parameters like tool radius, VSD, lubrication, rotational tool speed, feed rate and material thickness affects the formability and dimensional accuracy of the product [5-10]. Singh et al. [11] also justifies that the tool and lubrication have more influence in producing a sheet metal with better outputs. Kilani et al. [12] tried to improve the outputs of ISF process using a new rolling ball tool. Thinning of sheet, surface roughness, and forming force were taken for evaluation of the process and finally concluded that the newly designed tool gives better surface roughness compared to the hemispherical tool. Grimm et al. [13] proposed a new multi-directional tool with two hemispherical ends to increase the sheet metals formability and surface finish. The input factors by which the tool can make a positive effect was investigated. It was reported that this tool gives 23% formability improvement and a 21% spring back reduction.

[1] DEPARTMENT OF MECHANICAL ENGINEERING, DHANALAKSHMI SRINIVASAN UNIVERSITY, TIRUCHIRAPPALLI, TAMIL NADU, INDIA
[2] DEPARTMENT OF PRODUCTION ENGINEERING, NATIONAL INSTITUTE OF TECHNOLOGY, TIRUCHIRAPPALLI, TAMILNADU, INDIA
[3] DEPARTMENT OF MECHANICAL ENGINEERING, SAVEETHA SCHOOL OF ENGINEERING, SAVEETHA INSTITUTE OF MEDICAL AND TECHNICAL SCIENCES (SIMATS), CHENNAI

* Corresponding author: herbert.mech2007@gmail.com

Lu et al. [14] made a comparison between an oblique roller tool and existing hemispherical or ball ended tool based on the friction generated during the process. AA1100, AA2024, AA5052 and AA6111 were materials used for the experiment. After experimentation, the author found that the oblique roller tool offers better frictional effect compared to the existing tool. Therefore, the literature survey reveals that the work related to improving the formability and surface roughness of the sheet metal by designing a proper forming tool [28] has more scope. It is also noticed that the forming tool with multiple ball end does not exist in the literatures. Hence, the proposed work investigates the advantages of ISF process by using a newly designed multi-point tool having multiple ball ends which can make more number of mating points with the sheet metal. The multi-point tool consists of mandrel, hardened steel cup and balls. It has an outer diameter of 52 mm with the pitch diameter of 40 mm. It consists of totally six balls, each of diameter 12.7 mm. The balls are fixed at the bottom of the cup corner edge at an angle of 45° which helps to make a proper contact with the sheet metal. This multi-point tool also makes proper rolling contact which in turn improves the frictional effect between the tool and sheet metal. As this frictional effect helps to produce more shearing force which improves the ductility of the sheet metal [33]. Sometimes in single point tool the ball won't make proper rotation which may produce wear. This wear affects the surface quality of the sheet metal. Hence, the proposed tool makes an attempt to reduce this wear rate by using more number of balls. The sheet metal was formed to the shape hyperbolic truncated cone [15,20] since it helps more in forecasting the efficiency of both multi-point tool and single point tool. After forming process, the strain values of the formed sheet metals were procured using Video Measuring Machine (VMM). Through the obtained strain values, FLD and SD were plotted to observe the sheet metals formability. Bejaxhin et al. [29-31] have investigated the correlation of surface roughness and vibration analysis experimentally and it can be compared with the Deform 3D simulation platform. The stress induced during the process has been investigated in these researches. Suresh Kumar et al. [32] identified the die angle changes for the required angle leads to effective changes on Electro-chemical corrosion and tribological behaviour.

The SEM is also used to analyze the nature of fracture occurred during the forming process. Surface topography was made on the sheet metal using a non-contact measuring device such as SEM and 3D-Surface profilometer. These two analyses help to examine the ball marks produced by the tool over the sheet metal. The SEM image provides a focused view of the ball marks while the latter provides quantitative detail by means of light source. The Deform 3D tool is also used to forecast stresses, strain rate, and damage % using graphical outputs generated by SPIF and MPIF. The collected results were compared to the simulation results, assisting in the experimentation process. It can be aligned with the simulation part's borders.

2. Materials and methods

Owing to the desirable properties such as high quality, tensile behavior, elevated hardness and reasonable corrosion resistance of AISI 420 [16], it has been taken for experimentation with the thickness of 0.5 mm. Further its demand in oil, automobile and medical industry as valve, pressure equipments, surgical & dental equipments made to select this material. It also exhibits good working condition both in low and high temperature environments [17,18]. The sheet metal procured was sheared to a dimension of 150 mm × 150 mm which was then tightly fixed in the forming fixture using nut and bolt mechanism to avoid slipping of the sheet metal during forming process. Before experimentation, the material characteristics were studied using spectrometric analysis, metallographic analysis and tensile test. TABLE 1 shows the chemical composition of AISI 420 obtained through the spectrometric analysis.

TABLE1

AISI 420 chemical composition

	(% wt)							
Elements	**C**	**Mn**	**Cr**	**Ni**	**Mo**	**Si**	**P**	**Fe**
AISI 420	0.273	0.448	12.33	0.226	0.077	0.333	0.028	Rest

It contains a maximum of 12.33% of chromium content, which usually has the behavior of improving corrosion resistance and also acts as an oxidation agent. The carbon content contributes to the hardness of the material. In addition to these, a good percentage of manganese content was found (0.448%) which helps to improve the formability by providing better tensile strength. The strength and toughness of the material is improved by the presence of nickel content (0.226%). The yield strength and formability of the material is improved by phosphorous. Better elastic property and surface finish is possible by the silicon content of the material. This also helps in avoiding the fracturing at early stage. The molybdenum enhances the creep resistance of the material and slows down the fracture. The Fig. 1 portrays

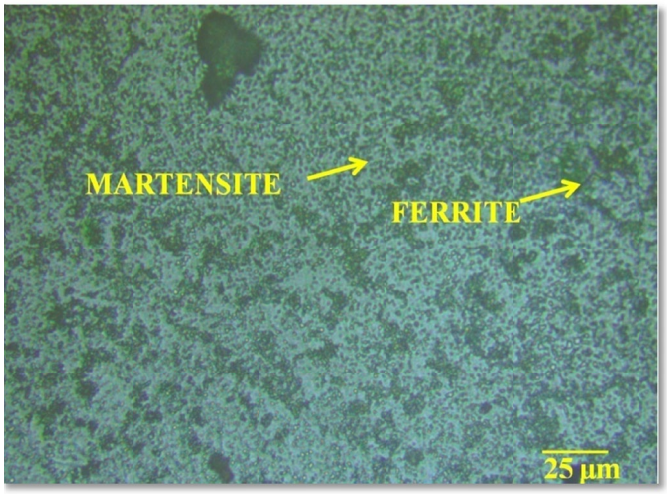

Fig. 1. Microstructure of AISI 420

the microstructure of the material which is obtained through metallographic analysis.

The dark spots on the microstructure of AISI 420 in Fig. 1, indicates the presence of carbide particles and, the rest (light) indicates ferrite phase. Then the tensile test was completed on the sheet metal using Universal Testing Machine (UTM) to obtain the strain hardening index of the materials. The sheet metal was sheared as per ASTM E08 standard and it is fixed in the UTM as shown in Fig. 2. As illustrated in Fig. 2, solid modelling programmes assist in the development of tool component models in the form of single point forming tool and multi-point forming tool. The solid model tools were created by employing correct dimensioning. This may be used to produce a metal specimen for the desired machining conditions in the top die position.

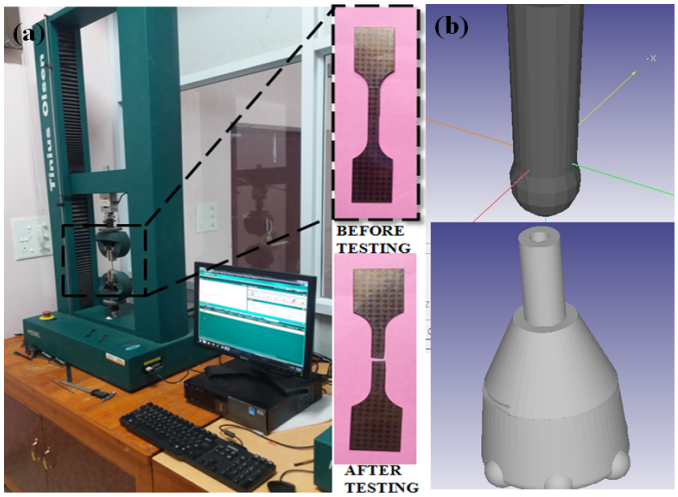

Fig. 2. (a) UTM setup used for tensile test and (b) Modelling of SPIF and MPIF

After testing, the measured values of engineering stress and engineering strain were substituted in true stress and true strain formula [19] to calculate the strain hardening index value (n). The value of n was calculated as 0.22. This lower strain hardening index value shows that, AISI 420 offers less resistance to tear in stretching process. It also resembles the results of spectrometric analysis represented in TABLE 1. After studying the properties of the AISI 420 using laser, the sheet was engraved with circular grids of 2 mm dimension and a gap of 1mm was maintained to get clarity while measuring the strain. The experimental process was carried out in a precision industry located at Thuvakudi, Tiruchirappalli. The vertical milling machine (Fig. 3a) was used for forming process in which both the fixture and the forming tools (single point & multi-point) were mounted to perform the variable angle test (Fig. 3b).The multipoint tool shown in the figure reveals how the ball is held in the multipoint tool. The ball is arrested by giving an extra projection in the sides of tool by drilling operation.

Based on the literature survey, the input parameters VSD 1.5 mm, feed 900 mm/min, speed 600 rpm were selected [19] and grease is used as lubricant. The experiment was prolonged until the sheet metal gets fractured and the repetitions of 4 experiments

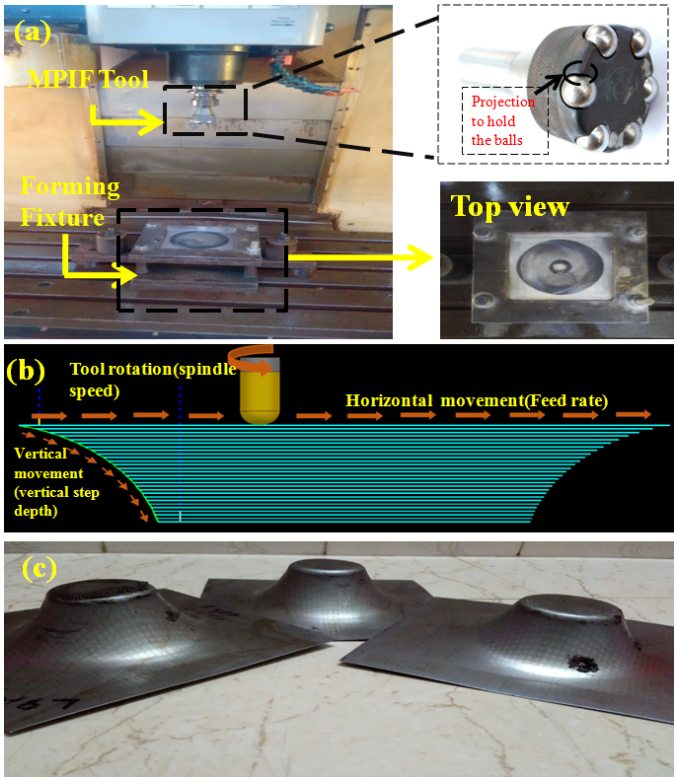

Fig. 3. Setup used for forming process: (a) Vertical milling machine used, (b) Tool movements with respect to various input parameters and (c) Sample sheets formed

were made in each tool to have a consistency in the work. After fracturing, the sheet metal was subjected to formability analysis using which the FLD and SD were obtained. Then the fractured portion was cut to the dimension of 10 mm ×10 mm to examine the nature of fracture occurred. Later, the sheet metal surface finish was viewed using SEM to get a qualitative analysis and the tests was extended with 3D-profilometer for a quantitative analysis. After investigations, the outcomes obtained through both the tools were compared.

3. Results and discussions

This section contains the results of the Formability, SEM analysis, Surface roughness analysis and Deform 3D prediction.

3.1. Formability analysis

Formability analysis predicts the plastic deformation capacity of the sheet metal. In this analysis, the grids around the fractured area were inspected to find the formability [26]. The circular grid marked over the sheet metal gets converted into elliptical grids during deformation as shown in Fig. 4.

From the elliptical grids, major and minor strain values were calculated by means of VMM and then the true strain values (major and minor) were calculated. The obtained strain values were plotted in the FLD graph to study the material behavior since it

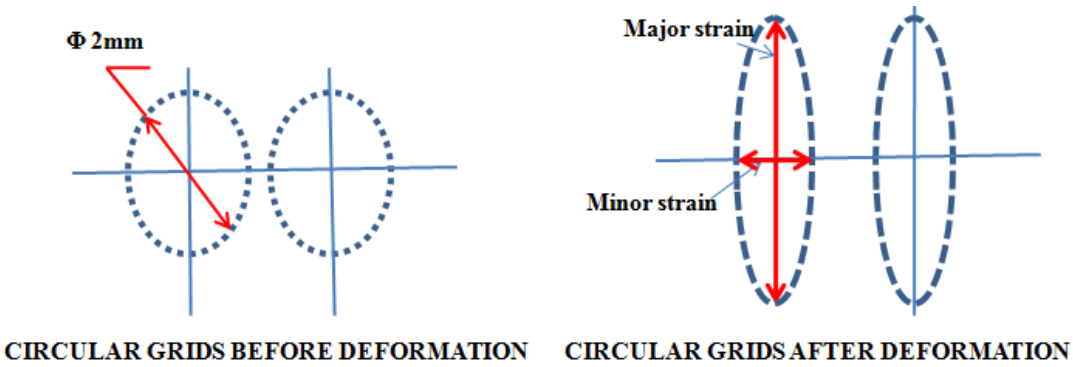

Fig. 4. Diagrammatic illustration of grid deformation

has more significance in predicting the fracture behavior during forming process [34]. It is also known that the strain limits of the sheet metals were reflected in the FLD. It consists of major and minor true strain value. Fig. 5 shows the FLD graph plotted by applying the major true strain values (ε_1) in *x*-axis and minor true strain (ε_2) in y-axis. The plotted strain values form a straight line falling from left to right with negative slope which indicate that the constant thickness strain condition with better formability is obtained at the fractured area [35]. It can also be seen from the FLD that the major true strain value attained through MPIF is greater than that of SPIF. Since AISI 420 has lesser *n* value [$n = 0.22$], it undergoes more work hardening effect during the stretching process. In SPIF, the tool applies more stress over a single point which impedes the plastic deformation [27]. As this material has more toughness due to the nickel content, giving more stress concentration on a single point may cause early fracture. Whereas the increased ball numbers in MPIF gives even stress over an increased area of the sheet metal. This helps in reducing the work hardening of the sheet metal and improves the formability. In addition, this material has considerable amount of phosphorous which enhance the formability of the material when proper stress is given. The FLD graph also shows that tension strain conditions evolved along the major axis of the grid during MPIF is higher. In addition to this a zigzag crack formed during the MPIF process is also shown in Fig. 5 which is usually formed when fracture is produced due to increased meridional stress [36].This meridional stress increase when tool-sheet metal contact is increased. This formability analysis continued with the SD by measuring the grids formed along the wall. Fig. 6 shows the measured strain values versus the distance of the grids measured along the formed surface. During MPIF the major strain values exhibits tension strain conditions and minor strain values undergoes compression strain conditions in accordance with the FLD.

Similarly in SPIF the tension and tension strain conditions can be observed in major and minor strain values. From the literature survey, it is noticed that the sheet metal producing tension-compression strain conditions during forming process produces better formability compared to the sheet metal producing tension-tension strain conditions [21]. So it can be justified that MPIF produces comparatively better formability without disturbing the ductility. Perhaps this may be due to the increased number of balls used in the multi-point tool. Also during SPIF the stress concentration will be subjected only to a particular mating point of the tool on the sheet metal, which in turn paves a path to earlier fracture. But in multi-point tool, the stress distributed through various mating points and helped to reduce the early fracture to a greater extent.

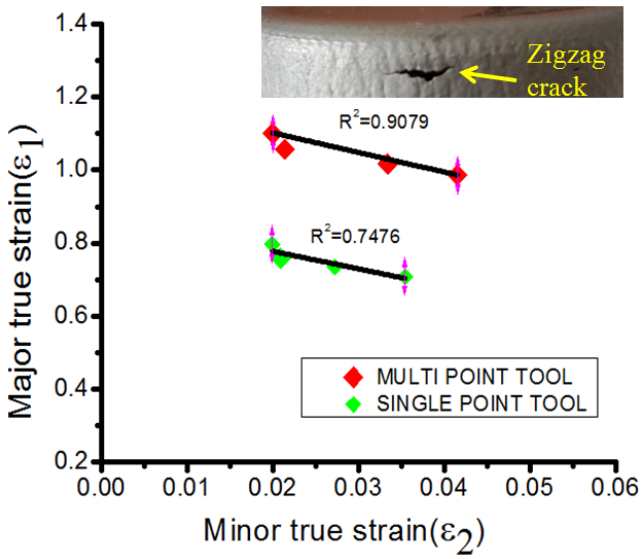

Fig. 5. FLD for the strain values obtained at the fractured area

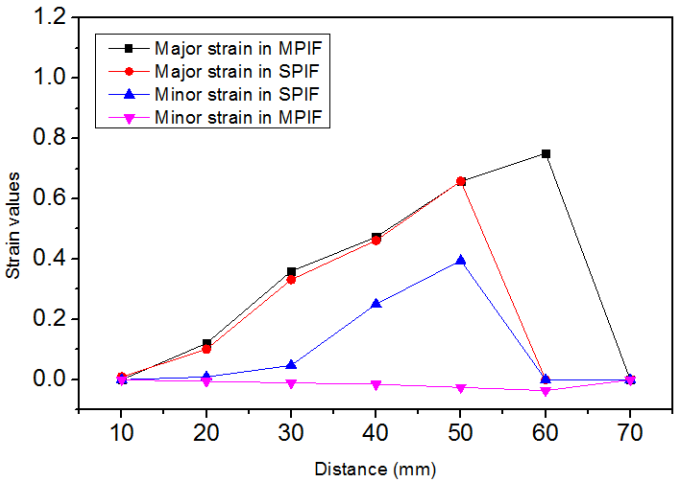

Fig. 6. Strain distributions measured over the sheet metal side walls

Further the sheet metal was looked in using SEM to find the fracture type. Usually ductile fracture happens when the fractured area contains more number of voids. Similarly, inter-granular cracking takes place when the fracture happens due to high stress [22]. The SEM images obtained from the cracked area of sheets created under MPIF and SPIF is given in Fig. 7 and Fig. 8 respectively. Increased number of micro-voids can be noticed in the SEM images of the sheet metal formed by MPIF. It shows that the sheet undergone more ductility which commensurate the FLD and SD outputs. The SEM images of the fractured area formed by using single point tool shows inter-granular fracture and facets formation is more. It justifies further that the stress formation in SPIF is higher [23] when compared to MPIF. Further the increased number of balls in multi-point tool improves the shearing action of the balls over the sheet metal, thus enhancing the shear stress during the forming process. The enhanced shearing stress helps out in producing a product under better ductile nature while forming.

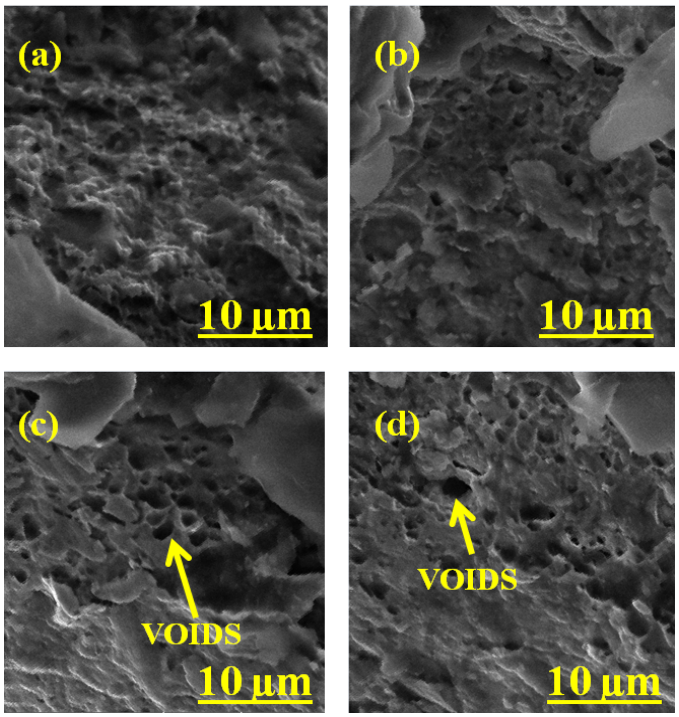

Fig. 7. SEM image of AISI 420 at cracked area during MPIF showing: (a), (b) Shear dimples formation, and (c), (d) Voids formation

3.2. Surface roughness analysis

Surface roughness analysis helps to compare the finishing of the product obtained from the MPIF and SPIF process. In addition to formability, specimen surface finish adds value to the product. As mentioned in spectrometric analysis the presence of silicon content (shown in TABLE 1) in the AISI 420 helps in the surface finish of the specimen. The large amount of chromium content also helps the tool to move smoothly over the surface of the sheet metal. The hardness of this material produced by the carbon content also helps to maintain the surface finish by resisting the scratches formed by the forming tool. The specimen was initially observed by SEM to examine the surface marks created by the balls during the MPIF and SPIF process. Fig. 9 shows the surface finish obtained through the process by MPIF & SPIF. In which Figs. 9a and 9b displays the surface finish of MPIF process and Figs. 9c & 9d displays the surface finish of SPIF process. From both the images it can be observed that

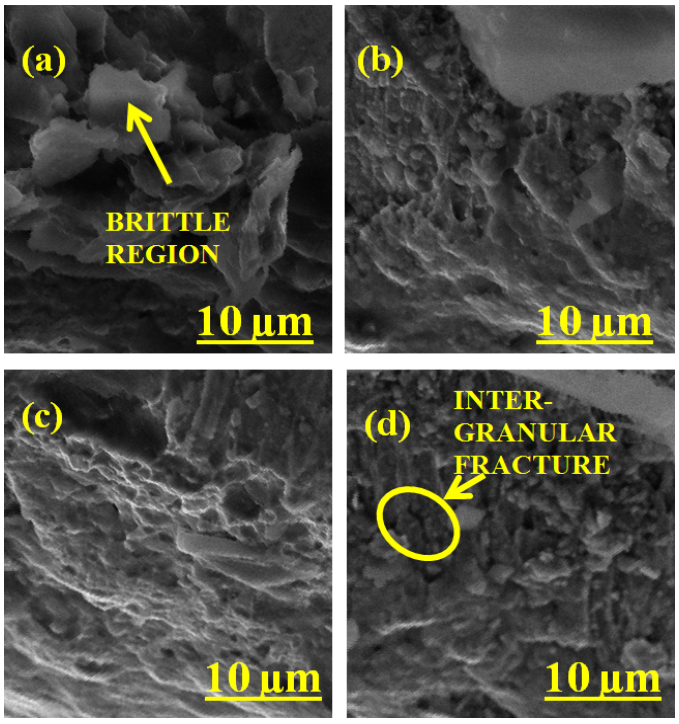

Fig. 8. SEM image of AISI 420 at cracked area during SPIF showing: (a), (b) Brittle regions (c), (d) Inter-granular fractures

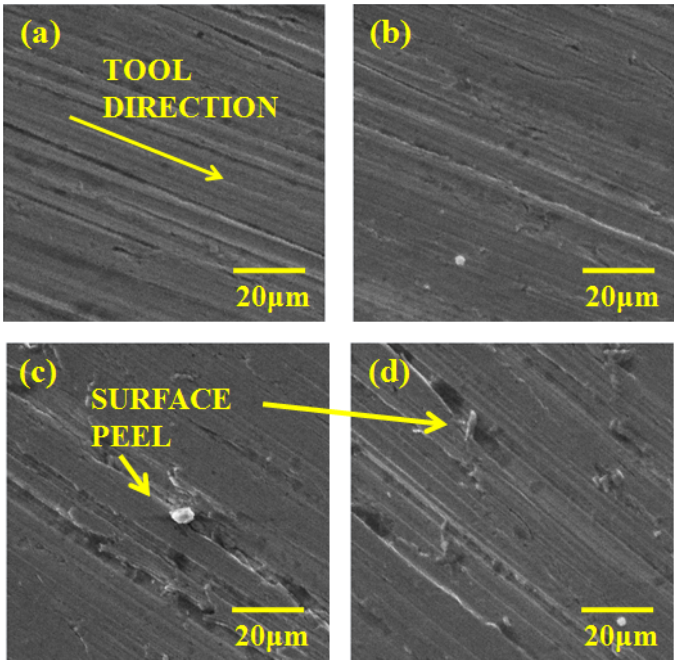

Fig. 9. SEM image obtained over the surface of the sheet metal formed during MPIF & SPIF: (c), (d) Tool marks created by multi-point tool, (c) Tear ridges formed by single point tool, and (d) Surface peel formed by single point tool

the tool mark made by multi-point tool is less compared to tool marks made by single point tool. Some tear ridges are observed in SEM images (Fig. 9c) of the specimen formed by single point tool. These tear ridges occur due to improper rotation of the tool and results irregular surface finish. Fig. 9c and Fig. 9d show that the surface of the specimen is peeled due to the improper rotation of the ball. This surface peel normally occurs due to the improper burnishing effect of the single point tool. Improper burnishing effect is created by the sliding effect of the tool over the sheet metal. Finally the sliding effect results tear and peel over the surface. These drawbacks could be avoided by ensuring proper rotation of the balls on the specimen. A closer observation was carried out on the sheet metal using the 3D-surface roughness profilometer. Fig. 10 displays the 3D-image of the surface finish obtained by MPIF and SPIF process. It shows that the SPIF process results more peaks and valleys than MPIF process. This may be due to the obstruction produced during the sliding action of the tool. The roughness plot given in Fig. 11 shows the peaks and valleys on the formed surface using SPIF are higher than those of MPIF. This roughness plot also justifies the results of 3D-roughness image. The better surface finish obtained by MPIF may be due to better ball rotation than SPIF process [24]. In addition to all these, work hardening may also be another reason for the surface roughness in specimen formed by SPIF. Increase in work hardening resists the plastic deformation and increases the surface asperities and thus producing a flake over the surface [25]. As said earlier, the work hardening is reduced by using more number of balls and the sliding effect created by the single point tool is rectified.

3.3. Prediction of performance through Deform 3D

The Deform 3D is a potent process simulation tool created by Scientific Forming Technologies Corporation to carry out the finite element analysis of the three-dimensional (3D) flow

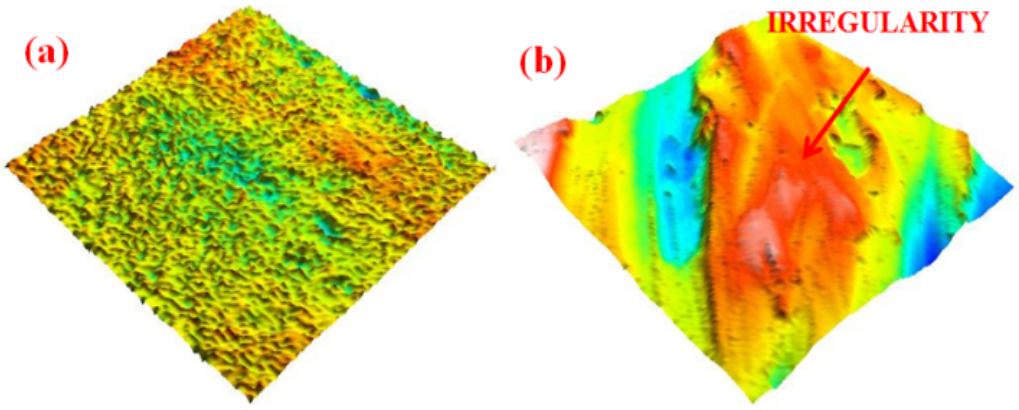

Fig. 10. 3D-Image of Surface finish obtained after (a) MPIF & (b) SPIF process

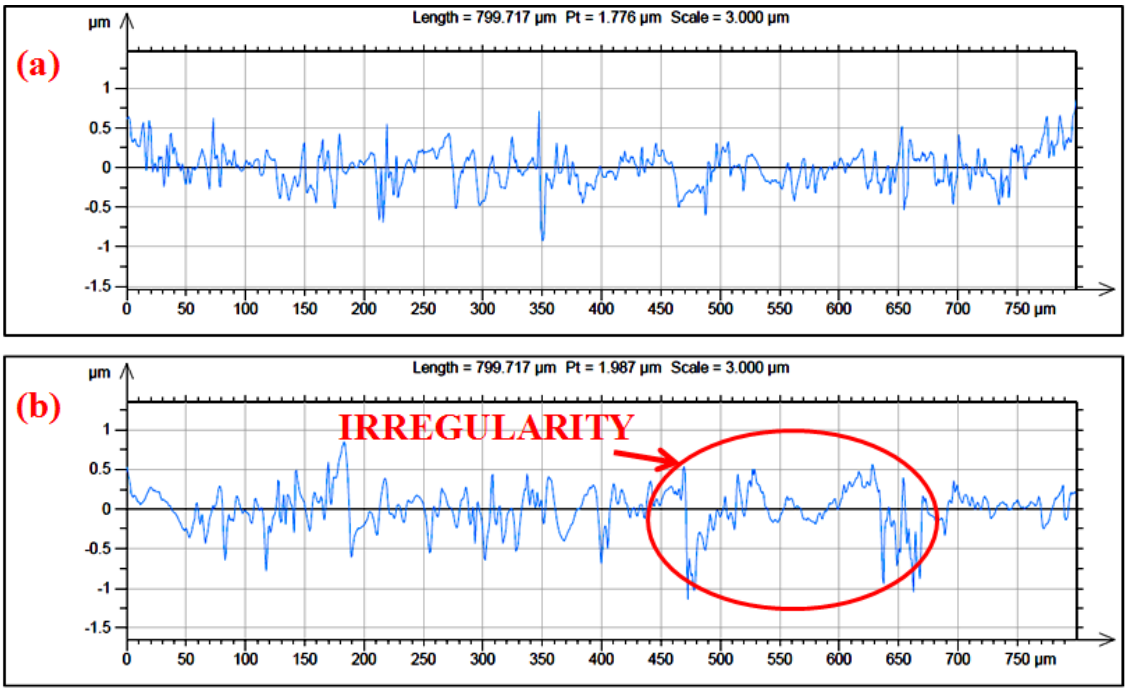

Fig. 11. Roughness plot obtained from sheet metal obtained after (a) MPIF and (b) SPIF process

of complicated metal forming processes. This programme was expanded to anticipate material flow during sheet metal forming even though it was originally designed for bulk forming processes like closed die and open die forging. Later, machining simulation for processes including turning, milling, boring, drilling, grooving and other operations was added to it. The superior prediction of stress concentrations which strongly connected to vibration and surface roughness was made possible by the use of Deform 3D. As demonstrated in Fig. 12, solid modelling aids in the development of the sepcimen model and assembled or dismantled form of experimental setup. The effective stress, velocity, boundary conditions, and percentage of damage have all been predicted using the multi-point forming tool, as given in Figs. 13a-d. This illustrates the results of each simulation of sheet metal forming operations using the multi-point tool, which can be compared to the existing single point forming tool. Before employing the velocity, damage, and effective stress output parameters, the performance of both tools can be estimated. The formability of an AISI 420 sheet metal specimen with a thickness of 0.5 mm and dimensions of 150 mm ×150 mm is excellent. Fig. 13 depicts the performance of the multi-point tool at the expected level, which can be satisfied in boundary level fixations (Fig. 13c). As shown in Fig. 13a and Fig. 13b, the boundary conditions are incorrectly defined and unbalanced with the fixed conditions of all four corners, and the displacement becomes zero (Fig. 13b). In this Deform 3D simulation, the boundary conditions have been applied to the specimen. The edges on both sides have been fixed and halted. Additionally, the specimen's bottom surface is totally anchored to the ground, making it impossible for it to move throughout the metal-forming operations. In the Deform 3D software application, this may be done using the boundary conditions section. Therefore, the boundary conditions' coordinate system has been used to account for the

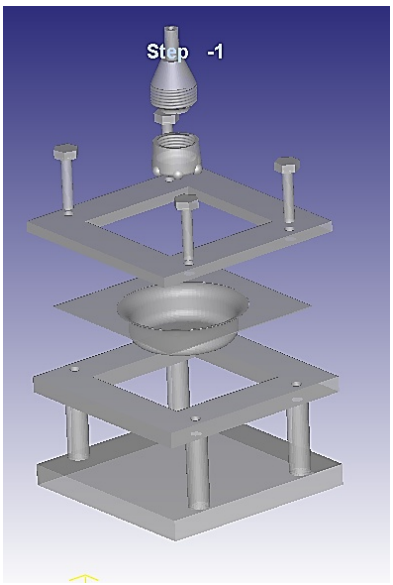

Fig. 12. Dismantled view of the specimen, forming tool and the fixture in Deform 3D

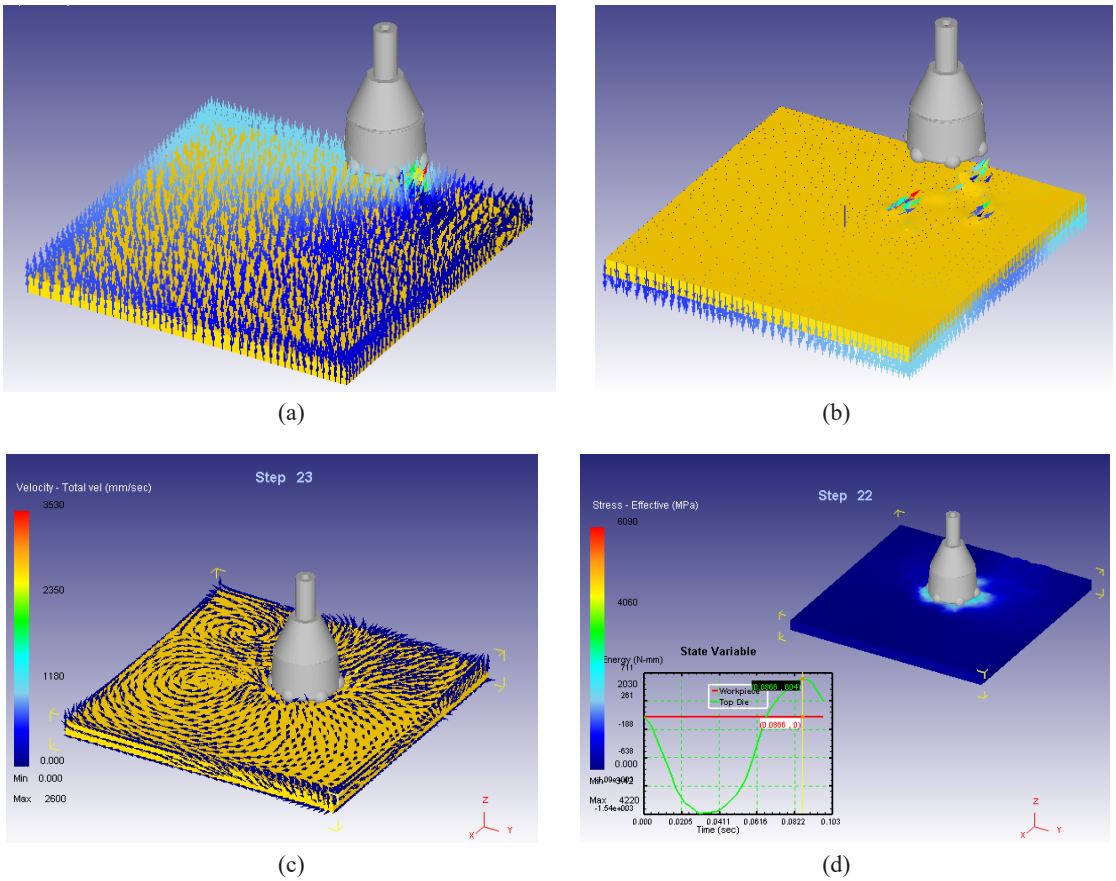

Fig. 13. (a)-(c) Predictions of boundary conditions, and (d) the stress and energy levels of multi-point forming tool with AISI 420

significant clamping effect caused by the fixation of all points (x, y and z) at each mesh node in the area where its constituent parts are meshed. The displacements for all of these fixed areas then equal zero. Consequently, both Figs. 13(a), (b), and (c). The slip line fields of the specimen's compressive zone can be used to expose the simulation findings, as described in the chapters by Nielsen and Martins [37] based on the deformation zone theory. The implicated specimen has been the subject of a subsequent mesh generation that has been started for this reason. Due to which the database generation activate the lagrangian approach of incremental formation. In the simulation techniques, there has been a stepwise iteration. The metal is formed during each iteration, and the values for stress, strain, and deformation may be determined using the energy levels shown in Figs. 13, 14, and 15. The conjugate gradient solver has used direct iterative methods to generate the deformation iteration steps.

As illustrated in Fig. 13c, our Deform 3D simulation platform has easily determined the boundary conditions from the velocity and total displacements. More discrepancies in the simulation results were detected based on the velocity components applied over the specifications and forming tool. The discrepancies can be fixed by applying suitably assigned boundary conditions of the forming specimen's corners and bottom surface. The complete arresting of the AISI 420 specimen was achieved by using the identical five displacment blocks illustrated in Fig. 13c. The von Mises stress has also been estimated for a constant depth of cut and homogeneous rotational speed and feedrate. It can be noted in Fig. 13d that the higher stress levels corresponding to the energy levels obtained for the state variables for the appropriate time duration. The vertical milling operation has been performed for this metal forming operation using SPIF and MPIF tools. Here, in these simulation procedures, the constitutive equation which is already present in the Deform 3D software for the milling simulation has been used for the metal forming operation which is also mentioned in Eq. (1). The constitutive equation for this simulative operation is

$$w = \int apVe^{-\frac{b}{T}} dt \tag{1}$$

Where p – interface pressure; V – Sliding velocity; T – Interface Temperature (Deg); dt – time increment; a, b – experimentally calibrated coefficients. Constitutive equations are mathematical relationships between two or more physical quantities. To define these mathematical relations, material constants, or coefficients unique to a material or a composite material, are needed. The constitutive equation, which is based on Hooke's law, explains the relationship between two physical qualities, such as the strain generated when stress exerted on a material with respect to time. For metal forming activities, the forming tool's vertical axis rotation is preferable. In order to create these simulation results using milling simulation control using the lagrangian incremental and conjugate gradient solver method.

Simulated results for single point forming tools have also provided better forecasts before machining. Following the defini-

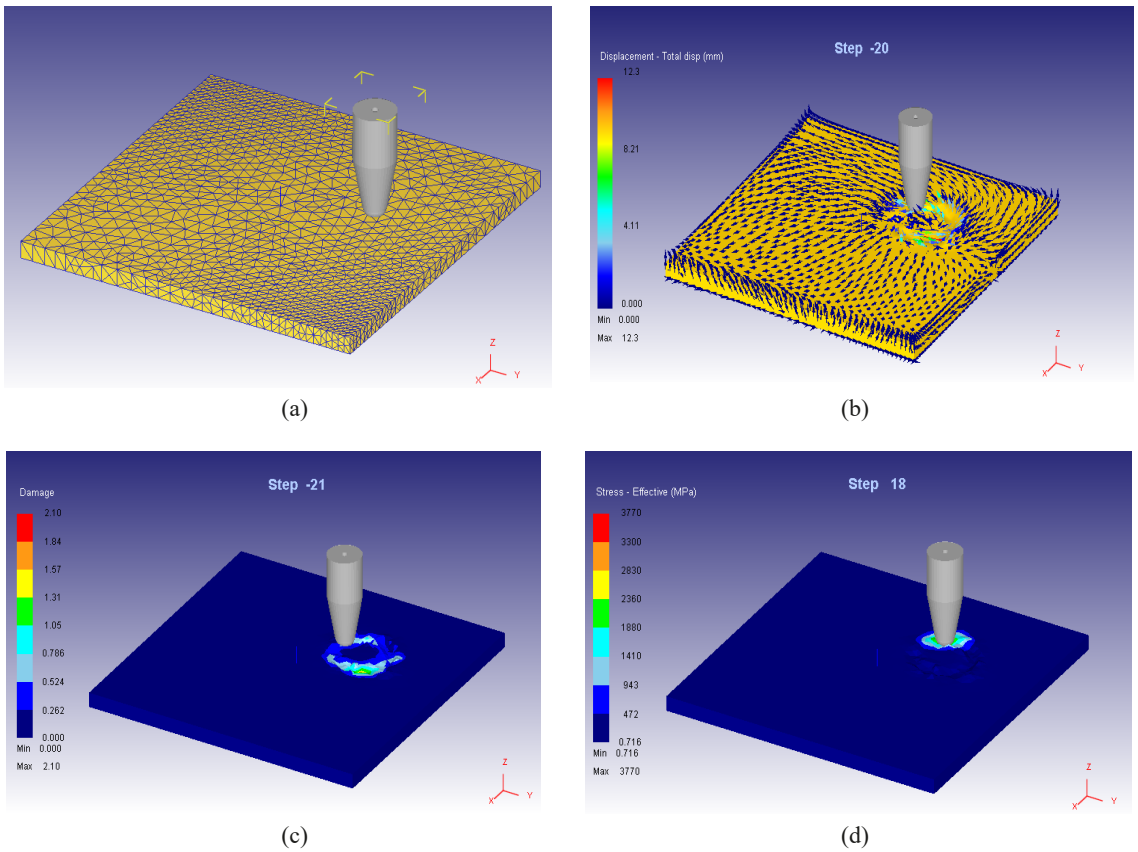

(a) (b)

(c) (d)

Fig. 14. (a), (b) Predictions of Mesh and velocity distribution, and (c), (d) Stress levels and damage percentage of Single point forming tool with AISI 420

tion of the safer boundary conditions, the single point forming tool was used to form the specimen at a forming speed and feed rate of 600 rpm and 900 mm/min for a forming depth of 1.5 mm, as illustrated in Fig. 14b. Fig. 14 shows how to simply calculate the percentage of damage from these Deform 3D simulations step by step (Fig. 14c). It is considered good if the percentage of damage is consistent throughout the forming process. It will be regarded bad forming if there are more variations from a constant damage percentage. As seen in Fig. 15, the single point forming tool has produced a non uniform percentage of damage, indicating a complex forming process over the specimen (Fig. 14b). However multi-point tool produces superior damage percentage data, as illustrated in Fig. 15a. In the simulation control for this metal forming procedure, the Deform 3D employing the lagrangian incremental method of iteration was used. From its material library, the suitable material composition has been specified for each top die and the work specimen material. The die stress analysis technique of simulation can be used at the simulation's post-processing step. Because of the ideal boundary conditions, no impacts can vary owing to the loading or unloading of the tool specimen model in this Deform 3D. We have merely fixed the tool movement path or travelling distance in any of the tool movement axes based on the assigned boundary conditions in the symmetry plane. In the post-processing step, the values of

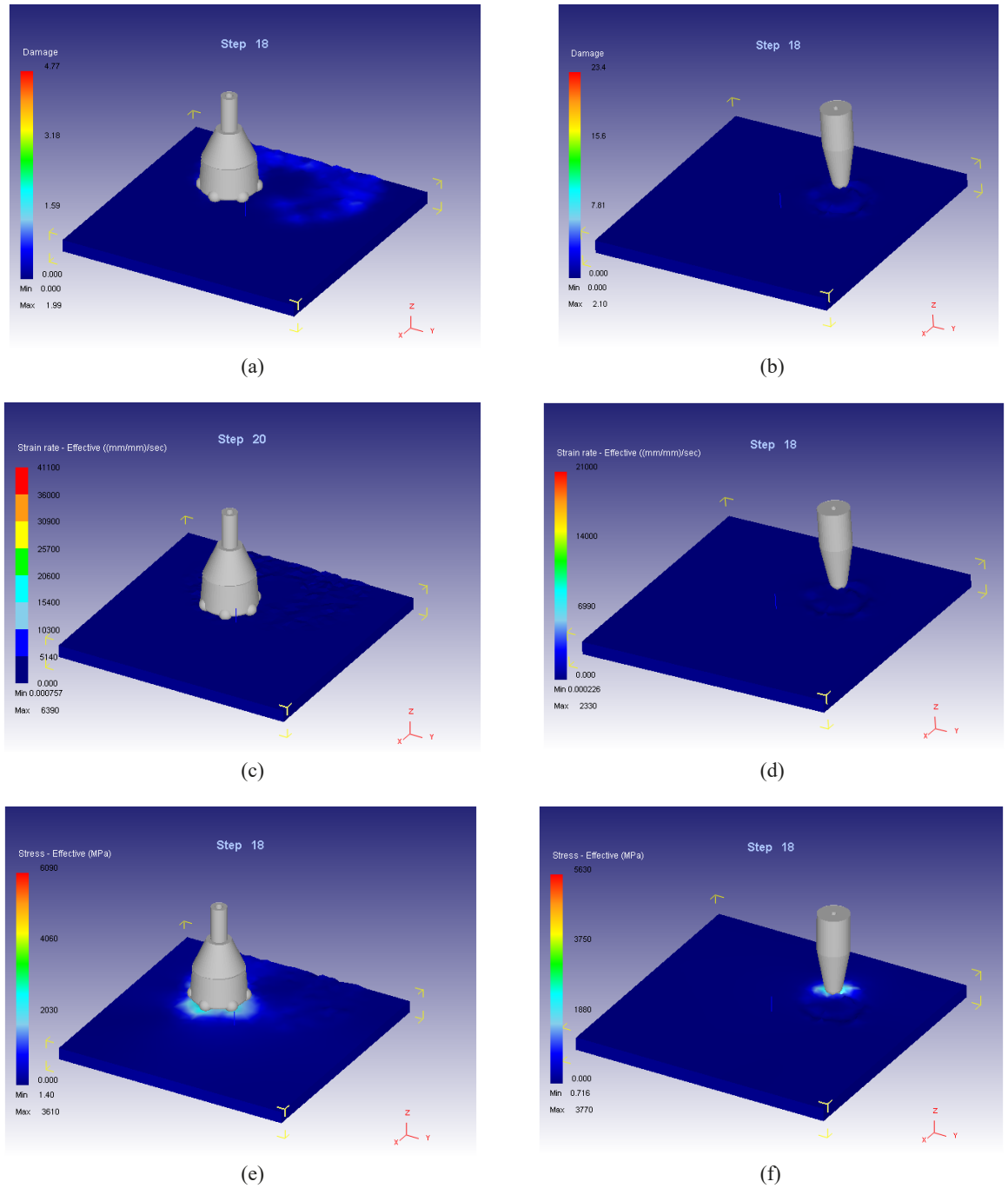

Fig. 15. (a) Damage rate during MPIF, (b) Damage rate during SPIF, (c) Effective strain rate during MPIF, (d) Effective strain rate during SPIF, (e) Effective stress rate during MPIF, and (f) Effective stress rate during SPIF

interaction such as tension and deformation between the tool and the specimen can be numerically expressed with any colour.

Various step numbers of 18 or 20 can be considered for distinction of stresses and strains during the iteration. Fig. 15c shows that the multi-point tool's strain rate reaches a maximum of 6390 per second, while the single point tool's strain rate is only 2330 per second. The plastic deformation level can be obtained by modest stresses and observed with reduced strain rates, according to the deformation theory. The lower cross section of single point forming tools can cover less area with lower strain rates, but the stress levels have been enhanced due to the single point forming tool's pointed action, as seen in Fig. 15e. Fig. 16 below shows the last stages of metal formation in their entirety. The deformation and stress levels at the later phases of metal forming are represented by this. The numbers 16 show the produced shape and its imprints. Based on the ultimate effort of the metal being formed by the tool components, the energy level with regard to time is also provided.

From these figures it can be noted that, because of the increased forming ball ends, the von Mises stresses have decreased during the forming stage with the multi-point tool, and the stress level can be equally distributed over the specimen with respect to the metal forming area. This justifies the above results obtained through experimental outputs like formability and surface roughness.

4. Conclusions

The study begins with the development of a new multi-point tool to provide better formability and surface finish to the final product. After completion of experimentation with the multi-point tool and single point tool, the outputs obtained are helping to predict the best tool. Comparison of formability was made by FLD, SD and SEM analysis. The formability analysis revealed that the mating points of multi-point tool help the formability improvement by enhancing the shearing action of tool. In addition, the roughness analysis made using SEM and 3D-surafce roughness tester compares the surface finish of the sheet metal formed. The SEM analysis clearly shows that the defects created by the single point tool are higher compared to multi-point tool and the same is further justified by using the results of 3D-image of the surface finish obtained latter. Therefore it shows that the better rotation of balls over the sheet metal improves the surface finish of the sheet metal. When compared to the SPIF tool, the MPIF forming method resulted in a lesser damage of 1.99 percent and an effective stress of 3610 MPa. The MPIF tool has also achieved the maximum strain rate, demonstrating improved metal forming qualities with fewer defects. Hence the results manifest that the multi-point tool gives better outputs compared to single point tool.

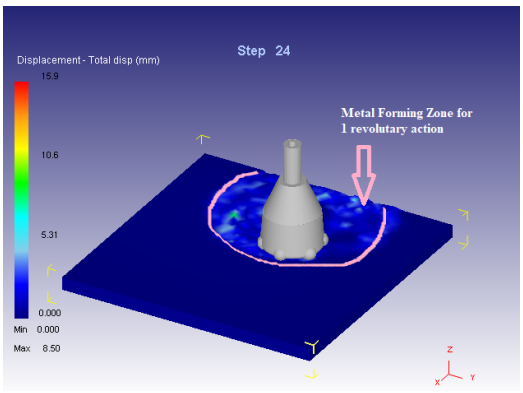

(a)

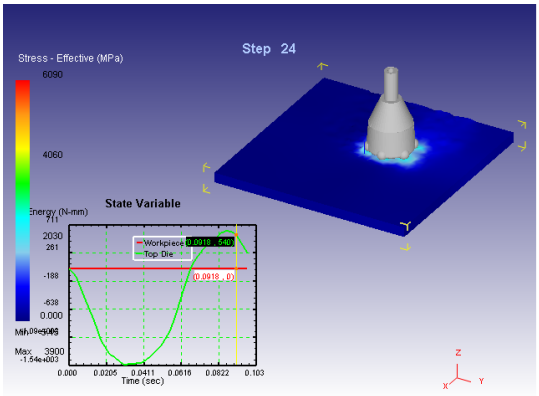

(b)

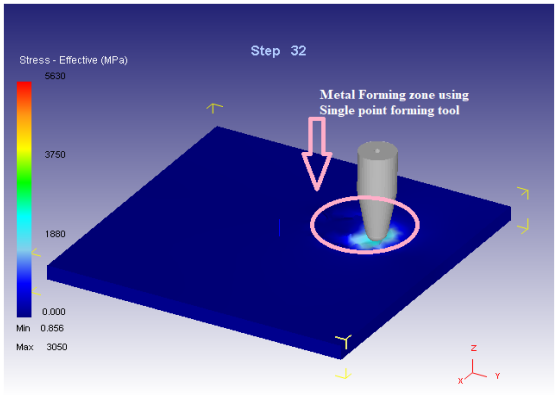

(c)

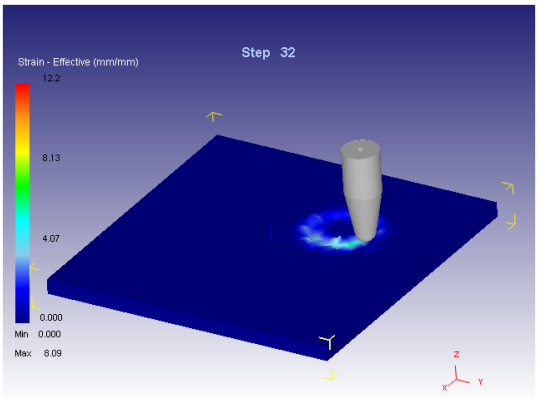

(d)

Fig. 16. Later stages (Step 24 and 32) of metal forming zones with various parameters (a) Deformation at metal forming zone (Step 24), (b) Von Mises Stress with energy levels of metal forming with respect to time (Step 24), (c) Metal forming zone using Single point forming tool (Step 32), (d) Strain effective outcome and clear metal forming zone (Step 32)

Conflict of interest

There is no conflict of interest.

REFERENCES

[1] F. Feng, J. Li, R. Chen, L. Huang, H. Su, S. Fan, Multi-point die electromagnetic incremental forming for large-sized sheet metals. J. Manuf. Process. **62**, 458-470 (2021).

[2] P. Chinnaiyan, A.K. Jeevanantham, Multi-objective optimization of single point incremental sheet forming of AA5052 using Taguchi based grey relational analysis coupled with principal component analysis. Int. J. Precis. Eng. Manuf. **15**, 2309-2316 (2014).

[3] M. Durante, A. Formisano, A. Langella, Observations on the Influence of Tool-Sheet Contact Conditions on an Incremental Forming Process. J. Mater. Eng. Perform. **20**, 941-946 (2011).

[4] M. Murugesan, D.W Jung, Formability and Failure Evaluation of AA3003-H18 Sheets in Single-Point Incremental Forming Process through the Design of Experiments. Materials **14**, 808 (2021).

[5] H. Ren, J. Xie, S. Liao, D. Leem, K. Ehmann, J. Cao, In-situ springback compensation in incremental sheet forming. CIRP Ann. Manuf. Technol. **68**, 317-320 (2019).

[6] H. Wei, L. Zhou, B. Heidarshenas, I.K. Ashraf, C. Han, Investigation on the influence of springback on precision of symmetric cone-like parts in sheet metal incremental forming process. Int. J. Lightweight Mater. Manuf. **2** (2), 140-145 (2019).

[7] F. Maqbool, M. Bambach, Dominant deformation mechanisms in single point incremental forming (SPIF) and their effect on geometrical accuracy. Int. J. Mech. Sci. **136**, 279-292 (2018).

[8] Z. Chang, J. Chen, Mechanism of the twisting in incremental sheet forming process. J. Mater. Process Tech. **276**, 116396 (2020).

[9] A. Fiorentino, C. Giardini, E. Ceretti, Application of artificial cognitive system to incremental sheet forming machine tools for part precision improvement. Precis. Eng. **39**, 167-172 (2015).

[10] L. Ben Said, J. Mars, M. Wali, F, Dammak, Effects of the tool path strategies on incremental sheet metal forming process. Mech. Ind. **17** (4), 411 (2016).

[11] S.A. Singh, S. Priyadarshi, P. Tandon, Exploration of Appropriate Tool Material and Lubricant for Elevated Temperature Incremental Forming of Aluminium Alloy. Int. J. Precis. Eng. Manuf. **22**, 217-225, (2021).

[12] L. Kilani, T. Mabrouki, M. Ayadi, H. Chermiti, S. Belhadi, Effects of rolling ball tool parameters on roughness, sheet thinning, and forming force generated during SPIF process,. Int. J. Adv. Manuf. Technol. **106**, 4123-4142 (2020).

[13] T.J. Grimm, R. Ihab, J.T. Roth, A Novel Modification to the Incremental Forming Process, Part 2: Validation of the Multi-directional Tooling Method. Procedia Manuf. **10**, 520-530 (2017).

[14] B. Lu, Y. Fang, D.K. Xu, J. Chen, H. Ou, N.H. Moser, J. Cao, Mechanism investigation of friction-related effects in single point incremental forming using a developed oblique roller-ball tool. Int. J. Mach. Tools. Manuf. **85**, 14-29 (2014).

[15] L. Bensaid, J. Mars, M. Wali, F. Dammak, Numerical prediction of the ductile damage in single point incremental forming process. Int. J. Mech. Sci. **131-132**, 546-558 (2017).

[16] A.N. Isfahany, H. Saghafian, G. Borhani, The effect of heat treatment on mechanical properties and corrosion behavior of AISI 420 martensitic stainless steel. J. Alloys Compd. **509**, 3931-3936 (2011).

[17] S.H. Baghjari, S.A.A. Akbari Mousavi, Effects of pulsed Nd:YAG laser welding parameters and subsequent post-weld heat treatment on microstructure and hardness of AISI 420 stainless steel. Mater. Des. **43**, 1-9 (2013).

[18] Z. Zhang, T. Yu, R. Kovacevic, Erosion and corrosion resistance of laser cladded AISI 420 stainless steel reinforced with VC. Appl. Surf. Sci. **410**, 225-240 (2017).

[19] C. Raju, C. Sathiya Narayanan, FLD and Fractography analysis of multiple sheet single point incremental forming. Trans. Indian. Inst. Metals **69**, 1237-1243 (2016).

[20] S. Gatea, B. Lu, J. Chen, H. Ou, G. McCartney, Investigation of the effect of forming parameters in incremental sheet forming using a micromechanics based damage model. Int. J. Mater. Form. **12**, 553-574 (2019).

[21] R. Narayanasamy, C. Sathiya Narayanan, Evaluation of limiting strains and strain distribution for interstitial free steel sheets while forming under different strain conditions. Mater. Des. **28**, 1555-1576 (2007).

[22] N.E. Dowling, Mechanical Behavior of Materials (4^{TH} Edition), 2013, Pearson Education Limited.

[23] G. Yoganjaneyulu, C. Sathiya Narayanan, R. Narayanasamy, Investigation on the fracture behavior of titanium grade 2 sheets by sing the single point incremental forming process. J. Manuf. Process. **35**, 197-204 (2018).

[24] M. Durante, A. Formisano, A. Langella, F.M.C Minutolo, The influence of tool rotation on an incremental forming process. J. Mater. Process Technol. **209** (9), 4621-4626 (2009).

[25] R. Azhiri, F. Rahimidehgolan, F. Javidpour, R.M. Tekiyeh, S.M. Moussavifard, A.S. Bideskan, Optimization of Single Point Incremental Forming Process Using Ball Nose Tool. Exp. Tech. **44**, 75-84 (2020).

[26] L. Ben Said, A. Bouhamed, M. Wali, B. Ayadi, S.A. Betrouni, H. Hajji, F. Dammak, SPIF Manufacture of a Dome Part Made of AA1060-H14 Aluminum Alloy Using CNC Lathe Machine: Numerical and Experimental Investigations. Arab. J. Sci. Eng. **46**, 12207-12220 (2021).

[27] A. Mulay, B. Satish Ben, S. Ismail, A. Kocanda, Experimental Investigation and Modeling of Single Point Incremental Forming for AA5052-H32 Aluminum Alloy. Arab. J. Sci. Eng. **42** (11), 4929-4940 (2017).

[28] S. Wu, P. Geng, N. Ma, F. Lu, Contact-induced vibration tool in incremental sheet forming for formability improvement of aluminum sheets. J. Mater. Res. Technol. **17**, 1363-1379 (2022).

[29] A. Bovas Herbert Bejaxhin, G. Paulraj, M. Prabhakar, Inspection of casting defects and grain boundary strengthening on stressed Al6061 specimen by NDT method and SEM micrographs. J. Mater. Res. Technol. **8**, 2674-2684 (2019).

[30] A. Bovas Herbert Bejaxhin, G. Paulraj, Effect of optimised cutting constraints by AlCrN/epoxy coated components on surface roughness in CNC milling. Int. J. Rapid. Manuf. **8**, 397-417 (2019).

[31] A. Bovas Herbert Bejaxhin, G. Paulraj, Experimental investigation of vibration intensities of CNC machining centre by microphone signals with the effect of TiN/epoxy coated tool holder. J. Mech. Sci. Technol. **33** (3), 1321-1331 (2019).

[32] P. Sureshkumar, T. Jagadeesha, L. Natrayan, M. Ravichadran, Dhinakaran Veeman, S.M. Muthu, Electrochemical corrosion and tribological behaviour of AA6063/Si3N4/Cu $(NO3)_2$ Composite processed using single-pass ECAPA route with 120° die angle. J. Mater. Res. Technol. **16**, 715-733 (2022).

[33] G. Yoganjaneyulu, C. Sathiya Narayanan, A comparison of fracture limit analysis on titanium grade 2 and titanium grade 4 sheets during single point incremental forming. J. Fail. Anal. Prev. **19**, 1286-1296 (2019).

[34] V. Panahizadeh, M. Hoseinpour, E. Gholamzadeh, M. Davoudi, Y. Dadgar Asl, Theoretical and experimental study of FLDs of AA5083 sheet and investigation of advanced anisotropic yield criteria coefficients. J. Braz. Soc. Mech. Sci. Eng. **44**, 356 (2022).

[35] M.B. Silva, P.S. Nielsen, N. Bay, P.A.F. Martins, Failure Mechanisms in Single Point Incremental Forming of Metals. J. Adv. Manuf. Technol. **56**, 893-903 (2011).

[36] M.B. Silva, M. Skjoedt, A.G. Atkins, N. Bay, P.A.F Martins, Single Point Incremental Forming & Formability/Failure Diagrams. J. Strain Anal. Eng. Des. **43**, 15-36 (2008).

[37] C.V. Nielsen, P.A.F Martins, Finite element simulation: A user's perspective. In: Metal Forming: Formability, Simulation and Tool Design, 2021, Academic Press, London.